JOURNAL OF SOLID STATE CHEMISTRY **139,** 213–219 (1998)
ARTICLE NO. SC977721

The Crystal Structures of Zr_5Te_4 and Zr_3Te

R. de Boer,*,[1] E. H. P. Cordfunke,* P. van Vlaanderen,* D. J. W. IJdo,† and J. R. Plaisier†

*Netherlands Energy Research Foundation ECN, P.O. Box 1, 1755 ZG Petten, The Netherlands, and †Leiden Institute of Chemistry, Gorlaeus Laboratories, Leiden University, P.O. Box 9502, 2300 RA, Leiden, The Netherlands

Received May 27, 1997; in revised form November 20, 1997; accepted November 24, 1997

In the zirconium-rich part of the Zr–Te system the stoichiometric compounds Zr_5Te_4 and Zr_3Te exist. The crystal structures of both compounds have been investigated. The crystal structure of Zr_5Te_4 has been resolved by Rietveld refinement of neutron powder diffraction data. It has a tetragonal body-centered unit cell with lattice parameters $a = 1.07649(6)$ nm, $c = 0.38403(3)$ nm, spacegroup *I4/m*, and is isostructural with Ti_5Te_4. The profile agreement factors are $R_p = 4.38\%$, $R_{wp} = 5.91\%$ and $S = 2.22$. The crystal structure of Zr_3Te has been resolved by Rietveld refinement of the X-ray powder diffraction data. It has a tetragonal body-centered unit cell with lattice parameters $a = 1.13382(6)$ nm and $c = 0.56265(5)$ nm, spacegroup $I\bar{4}$, isostructural with Ni_3P, with profile agreement factors $R_p = 12.5$, $R_{wp} = 13.6\%$ and $S = 1.06$. The structural similarities between both compounds are discussed. © 1998 Academic Press

***Key Words*: zirconium, tellurium, Zr_5Te_4, Zr_3Te, neutron powder diffraction, X-ray powder diffraction, lattice parameters, crystal structure, Rietveld refinement.**

1. INTRODUCTION

Tellurium is, as a precursor of iodine and due to its volatility, an important fission product (1). In the case of a severe nuclear reactor accident the release of tellurium partly determines the release of the radiotoxic iodine. Moreover, tellurium can in its elemental form easily be transported in the vapor phase through the primary cooling system of a reactor. During the initial stage of a reactor accident tellurium is released from the UO_2 fuel and will react with the inner surface of the Zircaloy cladding. Several zirconium–telluride compounds can be formed, and the formation of these compounds will cause significant retention of tellurium in the fuel cladding (2–4).

For reliable calculation of the tellurium release during accident conditions, it is of much importance to take into account the formation of zirconium–telluride compounds. Therefore, it is necessary to know which compounds exist in the Zr–Te system. A tentative phase diagram of the zirconium–tellurium system has recently been published (5). In nuclear accident consequence analysis the zirconium-rich tellurides are of particular interest, because the total amount of zirconium present in a reactor is much larger than the amount of tellurium. Brattås and Kjekshus (6) report that the Zr_5Te_4 is isostructural with Ti_5Te_4, but no structural details are known. The present work reports on the determination of the crystal structure of Zr_5Te_4 and Zr_3Te; their structural similarities are also discussed.

2. SYNTHESIS

For the preparation of Zr_3Te and Zr_5Te_4, zirconium powder (Cerac 99.7%, 34 ppm Hf, purified by heating at 900°C for 3 h in high vacuum to remove traces of ZrH_2) and tellurium powder (Merck 99%, purified by melting under a hydrogen/argon atmosphere to remove traces of TeO_2) were used.

For the synthesis of Zr_5Te_4, several mixtures of zirconium and tellurium powder with compositions between 0.60 and 0.54 mole fraction Zr, were heat treated in different manners to determine the composition of Zr_5Te_4 and the best way to prepare it. Zr_5Te_4 was finally prepared by the reaction of well mixed stoichiometric amounts of zirconium and tellurium powder in an evacuated and sealed quartz ampoule. The mixture was slowly heated for 2 days at 600°C. After the first heat treatment the reaction mixture was powdered, put into tungsten crucibles, and heated again under a purified argon atmosphere for 55 h at 1000°C, 80 h at 1100°C, and finally at 1200°C for 50 h. The final reaction product, a black powder that was unstable in air, consisted of Zr_5Te_4 and traces of hexagonal Zr and monoclinic ZrO_2. X-ray powder diffraction was used to determine the amounts of Zr and ZrO_2 impurities present in the samples. Therefore, several mixtures with varying compositions of Zr_5Te_4 and Zr and of Zr_5Te_4 and ZrO_2 were prepared by adding a weighed amount of Zr or ZrO_2 to a weighed amount of a sample of phase-pure Zr_5Te_4. The diffraction patterns of the sample and the mixtures were recorded simultaneously in different positions on the same film. The

[1] To whom correspondence should be addressed.

0022-4596/98 $25.00

intensities of the reflections of the impurities in the sample were compared visually with those of the mixtures. The composition of the mixtures was varied in such a way that the intensities of the reflections of the added impurities were identical to those in the sample. The amount of impurity in the sample was then considered to be equal to the amount of impurity in the mixture. In this way, the amount of mass fraction ZrO_2 in the sample was determined to be $(0.6 \pm 0.2) \times 10^{-2}$ and the mass fraction of Zr, $(3.0 \pm 0.5) \times 10^{-2}$.

For the synthesis of Zr_3Te, several mixtures of zirconium and tellurium powder with compositions between 0.85 and 0.67 mole fraction Zr were prepared. These mixtures were pelletized and placed separately in a tungsten crucible, which was heated for 2 h, under purified argon at 1200°C. The crucible was cooled and the reaction product, often a strongly sintered product, was powdered. Elemental analysis, using SEM/EDX (JEOL JXA 840) on a melted zirconium telluride sample, did not show contamination of the sample with tungsten. The composition of the reaction product was determined by weighing the reaction product before and after heating; weight loss during the reaction was solely caused by vaporization of tellurium. The X-ray powder diffraction pattern of samples of the condensed vapor corresponded to that of phase-pure tellurium (7). The weight loss was for all reaction mixtures less than 0.02 mass fraction of the total tellurium content. The reaction products were analyzed by X-ray powder diffraction. Coarse-crystalline Zr_3Te has a metallic luster and is, unlike Zr_5Te_4, stable in air.

All efforts to prepare phase-pure Zr_3Te led, however, to reaction products consisting mainly of Zr_3Te and small amounts of zirconium and/or Zr_5Te_4. The elemental zirconium present after reaction contained some tellurium in solid solution, as was concluded from the slight shift of the reflections in its diffraction pattern compared to the starting material. Since the reflections in the diffraction patterns of Zr_5Te_4 and Zr_3Te did not show detectable shifts for the various reaction mixtures, it is concluded that both compounds are line compounds.

All material handlings and storage of starting materials and reaction products were done under a purified–argon atmosphere to prevent any degradation of the zirconium telluride samples.

3. STRUCTURAL INVESTIGATION

3.1. Lattice Parameter Refinement

For accurate determination of the lattice parameters of Zr_5Te_4 and Zr_3Te, the X-ray powder diffraction patterns of samples with 0.430 and 0.167 mole fraction tellurium, respectively, were recorded on single-coated film with a focusing Guinier de Wolff camera (FR552, Enraf-Nonius, Delft, The Netherlands) using Cu$K\alpha_1$ radiation, $\lambda =$ 0.15405981(3) nm with α-SiO_2 (hexagonal, $a = 0.49133(2)$ nm, $c = 0.54053(4)$ nm) as an internal standard. The mole fractions are based on the masses of the starting materials.

Zr_5Te_4 has a body-centered tetragonal unit cell with lattice parameters $a = 1.07649(5)$ nm and $c = 0.38403(3)$ nm. The Smith and Snijder (8) figure of merit is: $F_{22} = 78$ (0.008, 35), range $2\theta = 11$–$68°$ (24 reflections of Zr_5Te_4 were observed, of which 22 were used for the lattice parameter refinement). The table with the d-values of the observed reflections of Zr_5Te_4 has been sent to the ICDD for inclusion in the PDF database. The lattice parameters of Zr_5Te_4, reported by Brattås and Kjekshus (6) ($a = 1.0763(2)$ nm, $c = 0.3840(1)$ nm), agree well with those obtained in the present study.

Zr_3Te also has a body-centered tetragonal unit cell with lattice parameters $a = 1.13382(6)$ nm and $c = 0.56265(5)$ nm. The Smith and Snijder (8) figure of merit for Zr_3Te is: $F_{30} = 94$ (0.008, 40), range $2\theta = 22$–$60°$ (35 reflections were observed, from which 30 were selected for the refinement). Reflections caused by the presence of hexagonal zirconium were subtracted from the observed diffraction pattern. The table with the *d*-values of the observed reflections of Zr_3Te has been sent to ICDD for inclusion in the PDF database. The lattice parameters recently reported by Harbrecht and Leersch (9) ($a = 1.1327(1)$ nm, $c = 0.56364(7)$ nm), deviate less than 0.2% from those obtained here. The body-centered tetragonal unit cell of Zr_3Te has an a/c ratio of 2.02, which is comparable to the a/c ratios of the body-centered tetragonal unit cells of Ni_3P (a/c = 2.04) and α-V_3S (a/c = 2.02), as reported by Aronsson (10) and Pedersen and Grønvold (11), respectively. Based on the systematic extinctions in the powder diffraction pattern ($h + k + 1 = 2n + 1$), no distinction could be made between the structure types. A Rietveld refinement of the structure of Zr_3Te (section 3.2.2) was therefore undertaken.

3.2. Rietveld Refinement of the Crystal Structures

3.2.1. Zr_5Te_4. Because no single crystals were available, Rietveld's method (12) was used for the refinement of the neutron powder diffraction data. A sample of about 14 grams of Zr_5Te_4 was used. Diffraction data were collected at room temperature on the powder diffractometer at the Petten High Flux Reactor in the angular range $2\theta = 5$–$155°$ in steps of 0.1°. The sample was placed in an airtight cylindrical sample holder (10 mm diameter, 100 mm height) made of vanadium closed with copper plugs fitted with Viton O-rings. Soller slits with a divergence of 30' were placed between the reactor and the monochromator and in front of the four ^{3}He counters. The wavelength of the neutrons was determined at $\lambda = 0.257117(4)$ nm after calibration with α-SiO_2.

The structure of Ti_5Te_4 (13) was used as the trial model. Following Weber (14), an absorption correction of $\mu R =$

0.07 was applied, and for the coherent scattering lengths, the value 7.16 fm for Zr and 5.80 fm for Te (15) were used. For the refinement of the neutron diffraction data the program DBW 9006, version 8.491 was used (16). The variables include a scale factor, six background parameters, three half width parameters defining the Gaussian-like peak shape, the zeropoint, an asymmetry parameter, the unit cell dimensions, atomic position parameters, thermal parameters, and a preferred orientation parameter (310). Scale factors for the small contributions of monoclinic ZrO_2 and hexagonal Zr were also refined. Details of the refinement are given in Table 1. The fractional atomic coordinates and isotropic thermal parameters of the atoms in Zr_5Te_4 are given in Table 2, and selected atomic distances are given in Table 3. The observed, calculated, and difference neutron powder diffraction patterns are shown in Fig. 1. Zr_5Te_4 has a calculated density, based on the lattice parameters determined with Guinier de Wolff analysis of $7.213\,g\cdot cm^{-3}$. The experimental density was measured picnometrically with double distilled CCl_4. A sample of $\sim 5g$ Zr_5Te_4 in a picnometer of $25\,cm^3$ volume was used. To prevent trapped voids in the polycrystalline sample, the measurements were done in vacuum. The experimental density was $7.21 \pm 0.05\,g\cdot cm^{-3}$.

3.2.2. Zr_3Te. To measure the powder diffraction pattern of Zr_3Te, a sample with 0.221 mole fraction tellurium (based on the masses of Zr and Te for the synthesis) and a PDS-120 diffractometer (Enraf-Nonius, Delft, The Netherlands) in Bragg-Brentano geometry, with a rotating sample holder and an INEL position sensitive detector were used. The diffractogram was measured at room temperature with Cu$K\alpha_1$ radiation, $\lambda = 0.1540598$ nm, in the angular range $2\theta = 2.5$–126° in steps of 0.03°. A 2θ correction of the observed pattern was applied, using the calculated 2θ values of the reflections of Zr_3Te. As a result, the lattice parameters of Zr_3Te were kept constant in the structure refinement.

The Ni_3P and the α-V_3S structure models were used for the Rietveld refinement of the crystal structure, with the FullProf 3.1 refinement program (17). This program is based on the original DBW3.2S program (16). The Ni_3P structure model, space group $I\bar{4}$ (82) turned out to be the correct one, giving final profile agreement factors $R_p = 12.5\%$, $R_{wp} = 13.6\%$, $R_e = 12.8\%$, and $S = 1.06$. These results were obtained by incorporating hexagonal zirconium as a second phase in the calculation of the diffraction pattern. The calculated lattice parameters of zirconium ($a = 0.32529(3)$ nm, $c = 0.51834(8)$ nm) were slightly higher than the lattice parameters of pure zirconium ($a = 0.3232$ nm, $c = 0.5147$ nm (18)). This difference may be caused by a small amount of tellurium dissolved in the zirconium lattice. Details of the structure refinement of Zr_3Te are given in Table 1. The observed, calculated, and difference powder diffraction pattern are shown in Fig. 2. The fractional coordinates and isotropic thermal parameters of the atoms in Zr_3Te are given in Table 4, and the calculated atomic distances in Table 5. The amount of sample of Zr_3Te was insufficient for a picnometrical determination of the density.

TABLE 1
Details of the Structure Refinement of Zr_5Te_4 and Zr_3Te

	Zr_5Te_4	Zr_3Te
Molar mass ($g\cdot mol^{-1}$)	966.52	401.27
a (nm) (X-ray)	1.07649(5)	1.13382(6)
(neutron)	1.07673(4)	
c (nm) (X-ray)	0.38403(3)	0.56265(5)
(neutron)	0.38407(2)	
V (nm^3) (X-ray)	0.44503	0.72331
Space group (Number)	$I4/m$ (87)	$I\bar{4}$ (82)
Z	2	8
$\rho_{calc.}$($g\cdot cm^{-3}$)	7.213	7.370
Data range ($^\circ 2\theta$)	5.0–155	2.5–126
Step size ($^\circ 2\theta$)	0.1	0.03
Wavelength (nm)	0.257117(4)	0.1540598
Number of data points	1501	4200
Number of variables	23	33
Impurities	Zr, ZrO_2	Zr
Peak profile	Gaussian	pseudo Voigt
R_p (%)	4.38	12.5
R_{wp} (%)	5.91	13.6
R_e (%)	2.69	12.8
S	2.22	1.06

TABLE 2
Fractional Atomic Coordinates and Isotropic Thermal Parameters of Zr_5Te_4 at Room Temperature, Space Group $I4/m$

Atom	Site	x	y	z	B (Å^2)
Zr(1)	a	0	0	0	0.17(6)
Zr(2)	h	0.3085(2)	0.3679(2)	0	0.17(6)
Te	h	0.0520(3)	0.2822(2)	0	0.70(7)

TABLE 3
Atomic Distances (nm) in Zr_5Te_4 at 298 K

Zr(1)	– 2 Zr(1)	0.38407(2)	Te	– Zr(1)	0.3091(2)
	– 8 Zr(2)	0.3156(2)		– Zr(2)	0.2912(4)
	– 4 Te	0.3091(2)		– 2 Zr(2)	0.2926(3)
				– 2 Zr(2)	0.2928(3)
Zr(2)	– 2 Zr(1)	0.3156(2)		– 2 Te	0.38407(3)
	– 2 Zr(2)	0.3551(3)		– 4 Te	0.3918(3)
	– 2 Zr(2)	0.38407(2)			
	– 2 Zr(2)	0.3414(3)			
	– 1 Te	0.2912(4)			
	– 2 Te	0.2926(3)			
	– 2 Te	0.2928(3)			

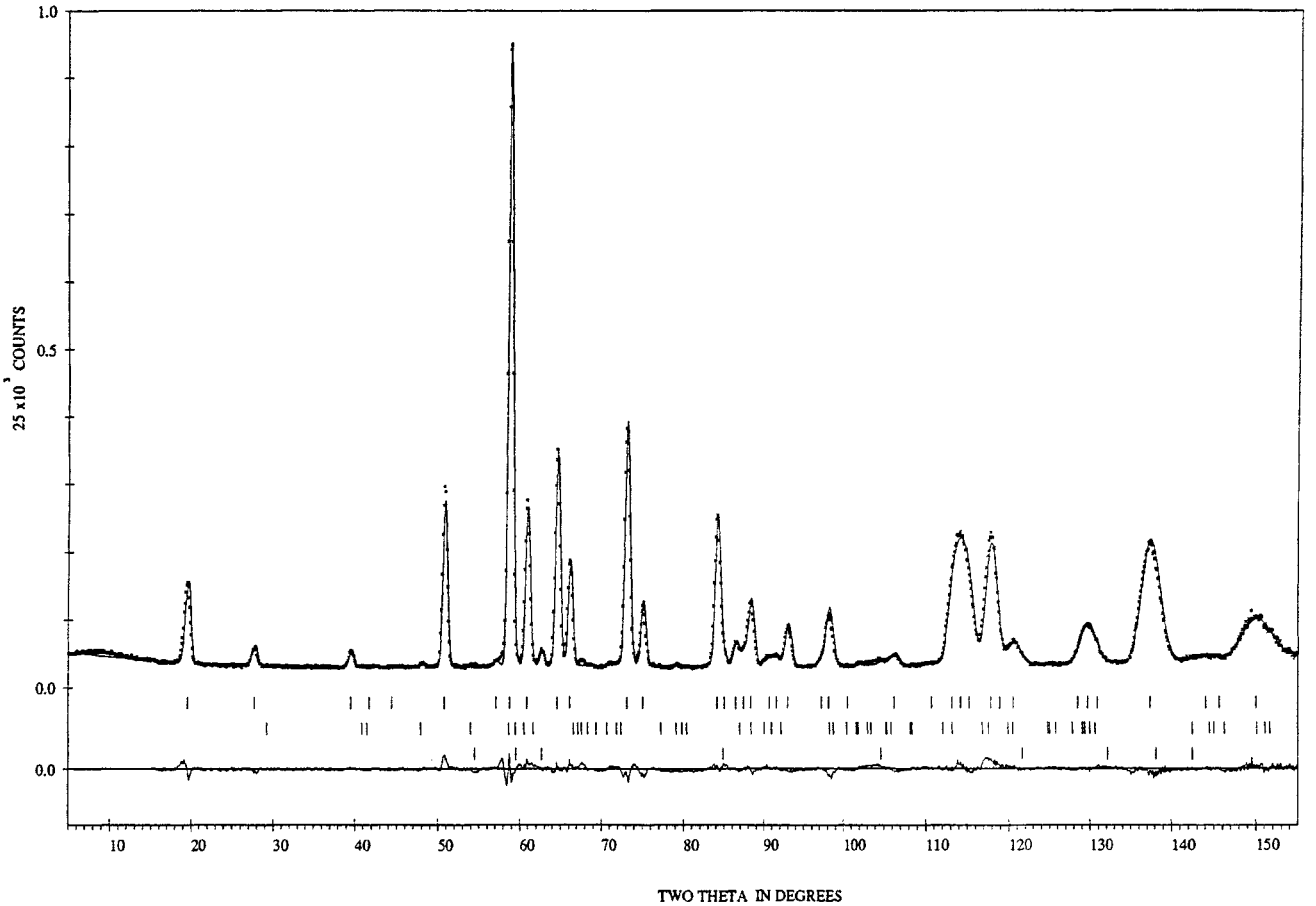

FIG. 1. Observed (dots) and calculated (solid line) neutron diffraction profiles of Zr_5Te_4. Tic-marks below the profile indicate the positions of the Bragg reflections of Zr_5Te_4 (top), ZrO_2 (middle), and Zr (bottom). Difference (observed–calculated) curve appears at the bottom of the plot.

4. DISCUSSION OF THE STRUCTURE

The crystal structure of Zr_5Te_4 is the same as that of Ti_5Te_4 (13). A projection of the structure along the c-axis is shown in Fig. 3. Zr_5Te_4 consists of quadratic columns of zirconium and tellurium atoms running parallel to the c-axis. Zr(1) is surrounded by four Te in a planar quadratic arrangement and by eight Zr(2) ($d[Zr(1)–Zr(2)] = 0.3156$ nm) in a prismatic, nearly cubic arrangement as in β-Zr ($d[Zr–Zr] = 0.3070$ nm). Zr(2) is surrounded by five tellurium atoms, four of them forming a rectangular arrangement, and further coordinated by two Zr(1) atoms and six Zr(2) atoms. Each Te atom is coordinated by six Zr atoms and six other Te atoms.

The crystal structure of Zr_3Te is of the Ni_3P type (10). A projection of the structure along the c-axis is shown in Fig. 4. The structure is built from columnar tetrahedra of $Zr(1)_4$ atoms, which run parallel to the c-axis through the origin and the center of the cells. Zr(3) covers the faces of the $Zr(1)_4$ tetrahedra. Zr(1) is surrounded by 12 zirconium and two tellurium atoms. The atomic distance in these dense-packed metal groupings ($d[Zr(1)–Zr(1)] = 0.303$ nm and $d[Zr(1)–Zr(3)] = 0.305$ nm) is even smaller than that in zirconium metal ($d[Zr–Zr]_{hex.} = 0.318$ nm). Zr(3) is surrounded by 10 Zr and three Te atoms. The Zr(2) atoms form a second tetrahedral column, parallel to the c-axis. The tellurium atoms are positioned on the faces of the $Zr(2)_4$ tetrahedra. Zr(2) is surrounded by 10 Zr and four Te atoms. Tellurium is surrounded by nine Zr atoms. The result of this structure refinement of Zr_3Te corresponds very well with the refinement recently reported by Harbrecht and Leersch (9), which was published after the completion of our structure determination.

The best results of the structure refinements of Zr_5Te_4 and Zr_3Te were obtained with equal occupancy of all atomic positions, indicating that both compounds are stoichiometric.

The structures of Zr_5Te_4 and Zr_3Te have significant similarities, which are clearly seen in a projection of the structures along the c-axis (Figs. 3 and 4). Both structures have diagonal planes in the unit cell, parallel to the c-axis, which are filled with Zr atoms. In Zr_5Te_4, tetrahedral columns of

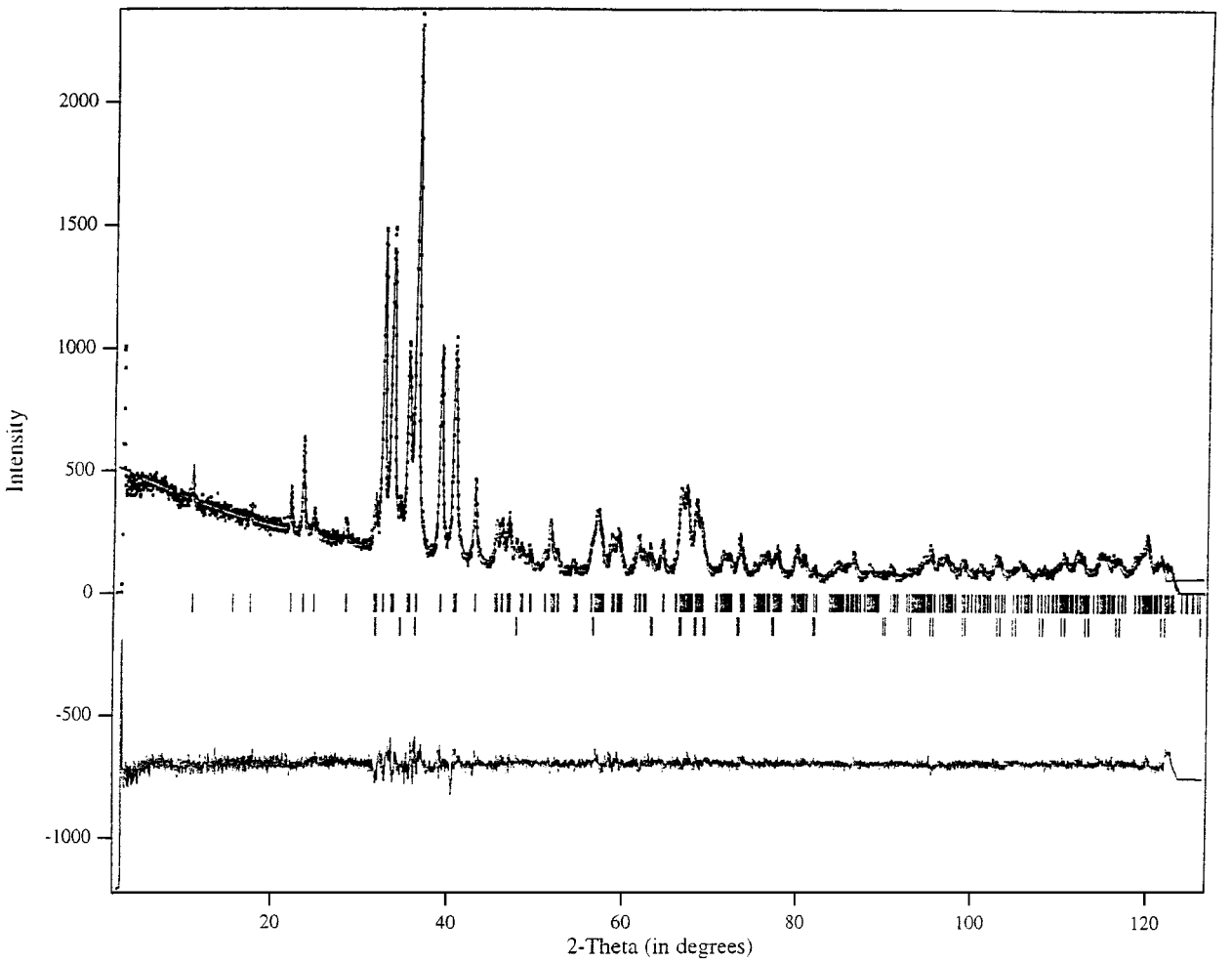

FIG. 2. Observed (dots) and calculated (solid line) X-ray diffraction profiles of Zr_3Te. Tic-marks below the profile indicate the positions of the Bragg reflections of Zr_3Te (top) and Zr (bottom). Difference (observed–calculated) curve appears at the bottom of the plot.

tellurium atoms parallel to the c-axis are located between these planes. In Zr_3Te, these tetrahedral tellurium columns are stacked together with tetrahedral columns of Zr(2) atoms. The structure of Zr_3Te thus arises from Zr_5Te_4 when additional zirconium atoms are inserted in the diagonal planes and the tetrahedral tellurium columns between the planes.

TABLE 4
Fractional Coordinates and Isotropic Thermal Parameters of the Atoms in Zr_3Te at 298.15 K, Space Group $I\bar{4}$

Atom	Site	x	y	z	B(Å^2)
Zr(1)	8g	0.0835(5)	0.1043(4)	0.2131(8)	0.5(1)
Zr(2)	8g	0.3574(3)	0.0184(4)	0.9817(11)	0.0(1)
Zr(3)	8g	0.1858(3)	0.2175(4)	0.7663(9)	− 0.26(9)
Te(1)	8g	0.2886(3)	0.0322(3)	0.4751(7)	− 0.01(7)

Although direct reaction of zirconium and tellurium occurs quite rapidly and at relatively low temperatures (< 800 K), only tellurium-rich compounds ($Zr_{1+x}Te_2$, $ZrTe_3$) are formed under these conditions (4). Reaction of a zirconium-rich mixture of Zr and Te at low temperature always leads to the formation of $Zr_{1+x}Te_2$ and an excess Zr metal. The mobilities of Zr and Te atoms in the solid state at moderate reaction temperatures are apparently too low to obtain chemical equilibrium. For the preparation of the zirconium-rich compounds Zr_5Te_4 and Zr_3Te, high reaction temperatures ($> 1200°C$) are necessary. Comparing the densities of the zirconium tellurides, it appears that the formation of Zr_5Te_4 from $Zr_{1+x}Te_2$ and Zr requires a strong increase in density of the material. The densities at room temperature of Zr and $Zr_{1+x}Te_2$ are approximately $6.5\,g\cdot cm^{-3}$; the density of Zr_5Te_4 is $7.21\,g\cdot cm^{-3}$. This indicates that an increase in density of more than 10% is necessary for the formation of Zr_5Te_4.

TABLE 5
Atomic Distances (nm) in Zr_3Te at 298.15 K

Zr(1)	– Te	0.2872(6)	Zr(3)	– Te	0.2908(6)
	– Te	0.3028(6)		– Te	0.2933(5)
	– Zr(1)	0.3030(7)		– Zr(1)	0.3051(7)
	– Zr(3)	0.3051(7)		– Te	0.3086(5)
	– Zr(1)	0.3215(7) (2×)		– Zr(2)	0.3144(6)
	– Zr(2)	0.3283(7)		– Zr(2)	0.3218(6)
	– Zr(3)	0.3319(7)		– Zr(3)	0.3253(7) (2×)
	– Zr(2)	0.3506(7)		– Zr(1)	0.3319(7)
	– Zr(3)	0.3537(7)		– Zr(2)	0.3432(7)
	– Zr(3)	0.3561(7)		– Zr(1)	0.3537(7)
	– Zr(3)	0.3624(7)		– Zr(1)	0.3561(7)
	– Zr(1)	0.3875(7) (2×)		– Zr(1)	0.3624(7)
Zr(2)	– Te	0.2888(7)	Te	– Zr(1)	0.2872(6)
	– Te	0.2900(5)		– Zr(2)	0.2888(7)
	– Te	0.2960(7)		– Zr(2)	0.2900(5)
	– Te	0.2962(5)		– Zr(3)	0.2908(6)
	– Zr(3)	0.3144(6)		– Zr(3)	0.2933(5)
	– Zr(3)	0.3218(6)		– Zr(2)	0.2960(7)
	– Zr(1)	0.3283(7)		– Zr(2)	0.2962(5)
	– Zr(3)	0.3432(7)		– Zr(1)	0.3028(6)
	– Zr(2)	0.3480(8) (2×)		– Zr(3)	0.3086(5)
	– Zr(1)	0.3506(7)			
	– Zr(2)	0.3798(8) (2×)			

Grønvold *et al.* (13) described the structural relation between $Ti_{1+x}Te_2$ (NiAs-structure type, $x = 0.6$) and Ti_5Te_4. The latter structure is obtained from $Ti_{1.6}Te_2$ when approximately 20% of the tellurium atoms are replaced by titanium atoms and vacancies in the structure are rearranged. This structural relation also holds for $Zr_{1+x}Te_2$ and Zr_5Te_4, since these structures are similar to the Ti–Te compounds.

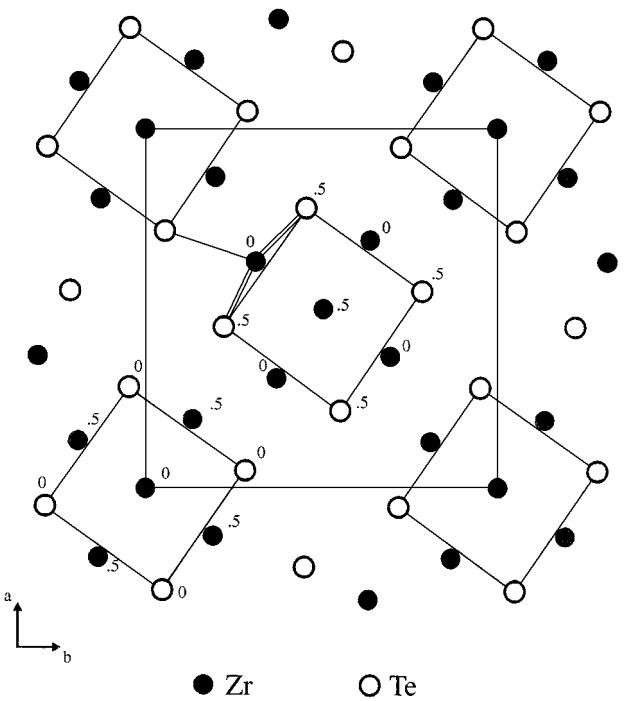

FIG. 3. Projection of the crystal structure of Zr_5Te_4 along the *c*-axis. The numbers indicate the *z*-parameter.

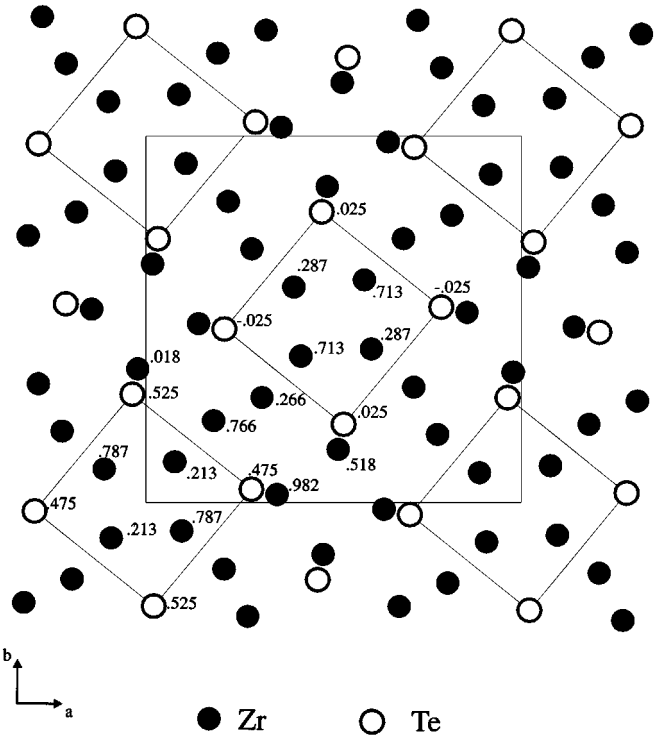

FIG. 4. Projection of the crystal structure of Zr_3Te along the *c*-axis. The numbers indicate the *z*-parameter.

Other transition metal-chalcogen compounds with a metal : chalcogen ratio of 5 : 4 adopting the Ti_5Te_4-type structure are found in the V–S, V–Se, Nb–Se, and Nb–Te systems (19). Transition metal-chalcogen compounds with a metal : chalcogen ratio of 3 : 1, which are isostructural with Ni_3P, were not found. Zr_3Sb and Zr_3Bi(19), however, are isostructural with Zr_3Te. V_3Te is the only transition metal-telluride other than Zr_3Te with a 3:1 composition, but no information about its structure is given (20). In the zirconium-rich parts of the Zr–Se and Zr–S systems, the compounds Zr_2Se(21) and Zr_2S(22) of the Ta_2P-type structure and Zr_3Se_2(23) of the WC-type structure are formed. The difference in structures of zirconium-rich sulphides and selenides compared to zirconium tellurides is probably caused by the more metallic character of tellurium compared to sulphur and selenium. In the Ti–Te system, a compound richer in titanium than Ti_5Te_4 was not found (24).

In the Hf–Te system, the presence of a compound Hf_3Te_2 is reported by Abdon and Hughbanks (25). Although the physical and chemical properties of Zr and Hf are almost equal and the composition of Hf_3Te_2 is intermediate between Zr_5Te_4 and Zr_3Te, its crystal structure is completely different. Hf_3Te_2 has a sandwich-like structure in which

layers of hafnium and tellurium are stacked–(Te–Hf–Hf–Hf–Te–) in a three-dimensional structure. At present, the reason for this remarkable difference in crystal structures between zirconium- and hafnium tellurides is not clear.

ACKNOWLEDGMENTS

Thanks to Annemiek Kok-Scheele for the preparation of Zr_5Te_4 and to Aad Bontenbal for the neutron powder diffraction measurements.

REFERENCES

1. D. J. Alpert, D. I. Chanin, and L. T. Ritchie, *Nucl. Saf.* **28**(1), 77 (1987).
2. J. L. Collins, M. F. Osborne, and R. A. Lorenz, *Nucl. Technol.* **77,** 18 (1987).
3. F. Garisto, report AECL 10691, 1992.
4. R. de Boer and E. H. P. Cordfunke, *J. Nucl. Mater.* **223,** 103 (1995).
5. R. de Boer and E. H. P. Cordfunke, *J. Alloys Compd.* **259,** 115 (1997).
6. L. Brattås and A. Kjekshus, *Acta Chem. Scand.* **25,** 2350 (1971).
7. JCPDS powder diffraction file 36–1452, International Center for Powder Diffraction Data, Pennsylvania, USA.
8. G. S. Smith and R. L. Snijder, *J. Appl. Crystallogr.* **12,** 60 (1979).
9. B. Harbrecht and R. Leersch, *J. Alloys Compd.* **238,** 13 (1996).
10. B. Aronsson, *Acta Chem. Scand.* **9,** 137 (1955).
11. B. Pedersen and F. Grønvold, *Acta Crystallogr.* **12,** 1022 (1959).
12. H. M. Rietveld, *J. Appl. Crystallogr.* **2,** 65 (1969).
13. F. Grønvold, A. Kjekshus, and F. Raaum, *Acta Crystallogr.* **14,** 930 (1961).
14. K. Weber, *Acta Crystallogr.* **23,** 720 (1967).
15. F. Sears, *Neutron News* **3,** 26 (1992).
16. D. B. Wiles and R. A. Young, *J. Appl. Crystallogr.* **14,** 149 (1981).
17. J. Rodriguez-Carvajal, "FULLPROF: A program for Rietveld Refinement and Pattern Matching Analysis," abstracts of the Satellite Meeting on Powder Diffraction of the XVth Congress of the IUCr, p. 127, Toulouse, France, 1990.
18. JCPDS powder diffraction file 5–665, International Center for Powder Diffraction Data, Pennsylvania, USA.
19. P. Villars and L.D. Calvert, "Pearson's Handbook of Crystallographic Data for Intermetallic Phases." ASM, Metals Park, Ohio, 1986.
20. E. Montigne, *Z. Anorg. Allg. Chem.* **362,** 329 (1968).
21. H. F. Franzen and L. J. Norrby, *Acta Crystallogr. Sect. B* **24,** 601 (1968).
22. B. R. Conard and H. F. Franzen, *High Temp. Sci.* **3,** 49 (1971).
23. H. Hahn and P. Ness, *Naturwissenschaften* **45,** 534 (1957).
24. H. Cordes and R. Schmid-Fetzer, *J. Alloys Compd.* **216,** 197 (1994).
25. R. L. Abdon and T. Hughbanks, *Angew. Chem.* **106,** 2414 (1994).